CORA Cork Open Research Archive
Cartlann Taighde Oscailte Chorcaí

Title	Large-area flexible colloidal photonic crystal film stickers for light trapping applications
Authors	Kohoutek, Tomas;Parchine, Mikhail;Bardosova, Maria;Fudouzi, Hiroshi;Pemble, Martyn E.
Publication date	2018
Original Citation	Kohoutek, T., Parchine, M., Bardosova, M., Fudouzi, H. and Pemble, M. (2018) 'Large-area flexible colloidal photonic crystal film stickers for light trapping applications', Optical Materials Express, 8(4), pp. 960-967. doi: 10.1364/OME.8.000960
Type of publication	Article (peer-reviewed)
Link to publisher's version	https://www.osapublishing.org/ome/abstract.cfm?uri=ome-8-4-960 - 10.1364/OME.8.000960
Rights	© 2018, Optical Society of America under the terms of the OSA Open Access Publishing Agreement
Download date	2024-10-12 03:53:48
Item downloaded from	https://hdl.handle.net/10468/5957

UCC
University College Cork, Ireland
Coláiste na hOllscoile Corcaigh

Research Article | Vol. 8, No. 4 | 1 Apr 2018 | OPTICAL MATERIALS EXPRESS 960

Optical Materials EXPRESS

Large-area flexible colloidal photonic crystal film stickers for light trapping applications

TOMAS KOHOUTEK,[1,*] MIKHAIL PARCHINE,[1] MARIA BARDOSOVA,[1] HIROSHI FUDOUZI,[2] AND MARTYN PEMBLE[1,3]

[1]*Tyndall National Institute, Lee Maltings, Dyke Parade, Cork, Ireland*
[2]*Colloidal Crystal Materials Group, National Institute for Materials Science, 1-2-1 Sengen, Tsukuba, 305-0047, Japan*
[3]*Department of Chemistry, University College Cork, College Road, Cork, Ireland*
**tomas.kohoutek@tndall.ie*

Abstract: We report on a way to make and transfer large-area (100 cm^2) free-standing 2D or 3D colloidal photonic crystal (CPC) films deposited using a roll-to-roll Langmuir-Blodgett technique from silica or polymer particles. Using this approach, a 'sticker' composed of a monolayer array of silica particles with 120 nm diameter in polyvinyl alcohol (PVA) glue was transferred onto a commercial flexible organic photovoltaic cell improving its conversion efficiency by some 5.2-8.3% at off-normal 0°-45° angles. The results presented here open up a range of new options for application of CPC films in the areas of photovoltaics and light-emitting devices.

© 2018 Optical Society of America under the terms of the OSA Open Access Publishing Agreement

OCIS codes: (240.0310) Thin films; (160.5298) Photonic crystals; (310.1210) Antireflection coatings.

References and links

1. J. E. G. J. Wijnhoven and W. L. Vos, "Preparation of photonic crystals made of air spheres in titania," Science **281**(5378), 802–804 (1998).
2. Q. Zhao, C. E. Finlayson, D. R. E. Snoswell, A. Haines, C. Schäfer, P. Spahn, G. P. Hellmann, A. V. Petukhov, L. Herrmann, P. Burdet, P. A. Midgley, S. Butler, M. Mackley, Q. Guo, and J. J. Baumberg, "Large-scale ordering of nanoparticles using viscoelastic shear processing," Nat. Commun. **7**, 11661 (2016).
3. H. Kim, J. P. Ge, J. Kim, S. E. Choi, H. Lee, H. Lee, W. Park, Y. D. Yin, and S. Kwon, "Structural colour printing using a magnetically tunable and lithographically fixable photonic crystal," Nat. Photonics **3**(9), 534–540 (2009).
4. H. Wang and K. Q. Zhang, "Photonic Crystal Structures with Tunable Structure Color as Colorimetric Sensors," Sensors (Basel) **13**(4), 4192–4213 (2013).
5. Z. Cai, N. L. Smith, J. T. Zhang, and S. A. Asher, "Two-Dimensional Photonic Crystal Chemical and Biomolecular Sensors," Anal. Chem. **87**(10), 5013–5025 (2015).
6. H. Fudouzi, T. Sawada, Y. Tanaka, I. Ario, T. Hyakutake, and I. Nishizaki, "Smart photonic coating as a new visualization technique of strain deformation of metal plates," Proc. SPIE **8345**, 83451S (2012).
7. M. Karg, T. A. F. Konig, M. Retsch, C. Stelling, P. M. Reichstein, T. Honold, M. Thelakkat, and A. Fery, "Colloidal self-assembly concepts for light management in photovoltaics," Mater. Today **18**(4), 185–205 (2015).
8. G. Kocher-Oberlehner, M. Bardosova, M. Pemble, and B. S. Richards, "Planar photonic solar concentrators for building-integrated photovoltaics," Sol. Energy Mater. Sol. Cells **104**, 53–57 (2012).
9. E. Armstrong and C. O'Dwyer, "Artificial opal photonic crystals and inverse opal structures – fundamentals and applications from optics to energy storage," J. Mater. Chem. C Mater. Opt. Electron. Devices **3**(24), 6109–6143 (2015).
10. P. Jiang, J. F. Bertone, K. S. Hwang, and V. L. Colvin, "Single-Crystal Colloidal Multilayers of Controlled Thickness," Chem. Mater. **11**(8), 2132–2140 (1999).
11. Y. Fang, B. M. Phillips, K. Askar, B. Choi, P. Jiang, and B. Jiang, "Scalable bottom-up fabrication of colloidal photonic crystals and periodic plasmonic nanostructures," J. Mater. Chem. C Mater. Opt. Electron. Devices **1**(38), 6031–6047 (2013).
12. M. Bardosova, M. E. Pemble, I. M. Povey, and R. H. Tredgold, "The Langmuir-Blodgett Approach to Making Colloidal Photonic Crystals from Silica Spheres," Adv. Mater. **22**(29), 3104–3124 (2010).
13. M. Parchine, J. McGrath, M. Bardosova, and M. E. Pemble, "Large Area 2D and 3D Colloidal Photonic Crystals Fabricated by a Roll-to-Roll Langmuir-Blodgett Method," Langmuir **32**(23), 5862–5869 (2016).
14. X. Yan, J. Yao, G. Lu, X. Chen, K. Zhang, and B. Yang, "Microcontact Printing of Colloidal Crystals," J. Am. Chem. Soc. **126**(34), 10510–10511 (2004).

#313617 https://doi.org/10.1364/OME.8.000960
Journal © 2018 Received 15 Nov 2017; revised 14 Jan 2018; accepted 15 Jan 2018; published 20 Mar 2018

Optical Materials EXPRESS

15. W. Li, B. Yang, and D. Wang, "Fabrication of Colloidal Crystals with Defined and Complex Structures via Layer-by-Layer Transfer," Langmuir **24**(23), 13772–13775 (2008).
16. A. Yadav and M. S. Tirumkudulu, "Free-standing monolayer films of ordered colloidal particles," Soft Matter **13**(25), 4520–4525 (2017).
17. H. Fudouzi, "Colloidal Photonic Crystal Films: Fabrication and Tunable Structural Color and Applications," In *Nanomaterials and Nanoarchitectures,* NATO Science for Peace and Security Series C: Environmental Security, M. Bardosova, T. Wagner, eds. (Springer, 2015).
18. T. Kohoutek, J. Orava, L. Strizik, T. Wagner, A. L. Greer, M. Bardosova, and H. Fudouzi, "Large-area inverse opal structures in a bulk chalcogenide glass by spin-coating and thin-film transfer," Opt. Mater. **36**(2), 390–395 (2013).
19. I. Mathews, D. O'Mahony, K. Thomas, E. Pelucchi, B. Corbett, and A. P. Morrison, "Adhesive bonding for mechanically stacked solar cells," Prog. Photovolt. Res. Appl. **23**(9), 1080–1090 (2015).
20. W. C. Luk, K. M. Yeung, K. C. Tam, K. L. Ng, K. C. Kwok, C. Y. Kwong, A. M. C. Ng, and A. B. Djurisic, "Enhanced conversion efficiency of polymeric photovoltaic cell by nanostructured antireflection coating," Org. Electron. **12**(4), 557–561 (2011).
21. A. Deak, B. Bancsi, A. L. Toth, A. L. Kovacs, and Z. Horvolgyi, "Complex Langmuir–Blodgett films from silica nanoparticles: An optical spectroscopy study," Colloid Surf. A **278**(1-3), 10–16 (2006).

1. Introduction

Colloidal photonic crystal (CPC) structures [1] including colloidal photonic crystal thin films have been recently developed in number of promising applications by employing their stimuli-responsive stop-band structures and structural color, e.g. as photonic fabrics [2], magnetic displays [3], optical sensing [4–6], enhanced photovoltaics [7,8] or in energy storage [9].

CPC growth via self-assembly of colloidal monodisperse spheres of dielectric materials involves various fabrication methods such as controlled evaporation [10] spin coating [11], shear growth [2], the Langmuir–Blodgett (LB) method [8,12,13] and others. It is fair to note here that despite fairly continuous progress in the development of these materials and their applications, there are still some fundamental issues linked specifically with the various deposition routes that have not been solved completely, i.e. lack of control over the fabrication process and the lack of scale-ability toward high volume manufacturing, which are currently limiting the widespread use of these materials.

Among the many CPC assembly techniques, the LB method represents one of the fastest, most versatile and most scalable approaches for deposition of high quality two-dimensional and three-dimensional colloidal photonic crystal films. The options of being able to control the number of deposited layers in a layer-by-layer process, the ability to choose different particle sizes for each deposited layer, and the progress in LB roll-to-roll processing on flexible substrates reported recently [13], represent important achievements which have brought these materials and the associated LB technology much closer to practical use.

Considering the potential applications of large area CPCs such as in enhancing the performance of thin film photovoltaics or flexible OLEDs, it is desirable to be able to control not only the optical properties but also their mechanical properties so as to facilitate their easy application to the structure in question since of these materials on real-size devices demand a certain level of robustness. In this regard CPCs [2,3,8] developed for certain applications take the physical form of a composite in which an array of self-assembled polymer or silica nanoparticles is responsible for the optical effect, e.g. stop-band formation, while the polymer cross-linker secures the required mechanical and chemical properties.

Composite CPCs made of materials such as silica and polymers embedded in other polymers with typical refractive index values in the range of 1.44-1.60 necessarily have lower refractive index difference and thus decreased amplitude of the optical effects than the original colloidal photonic crystal films which still possess void spaces filled with air ($n_{air} \approx 1$). The design of the CPC films for real applications then has to balance the overall material properties while keeping the amplitude of the optical effects at an exploitable level.

In this paper, we demonstrate a simple way to make and transfer large-area colloidal crystal photonic films assembled from silica and polymer nanoparticles onto new surfaces via

Optical Materials EXPRESS

the formation of a composite with commercially available PVA glue which effectively takes the form of freestanding sticker. We argue that the development of a simple, cheap, post processing transfer method such as this opens up the use of these materials for the general improvement in performance of in a wide range of optical devices. The CPC / PVA films allowed for complete transfer of samples with over than 100 cm^2 surface areas. An example shows the antireflective effects of a LB monolayer of silica particles with 120 nm diameter embedded in PVA transferred onto a commercial organic photovoltaic cell enhancing its conversion efficiency by about 5.2-8.3% measured at various angles in comparison with the diffractive effects obtained by using a LB monolayer of silica particles with 740 nm diameter in PVA instead.

2. Experimental

The particle chemistry, including synthesis and characterization as well as the parameters of the roll-to-roll LB deposition process used in order to fabricate the CPC films has been reported previously [13]. The fabrication route is currently capable of making high-quality LB mono and multilayers on flexible polyester (PES) including substrates of up to 500 cm^2 surface area on the roll with the width of 10 cm.

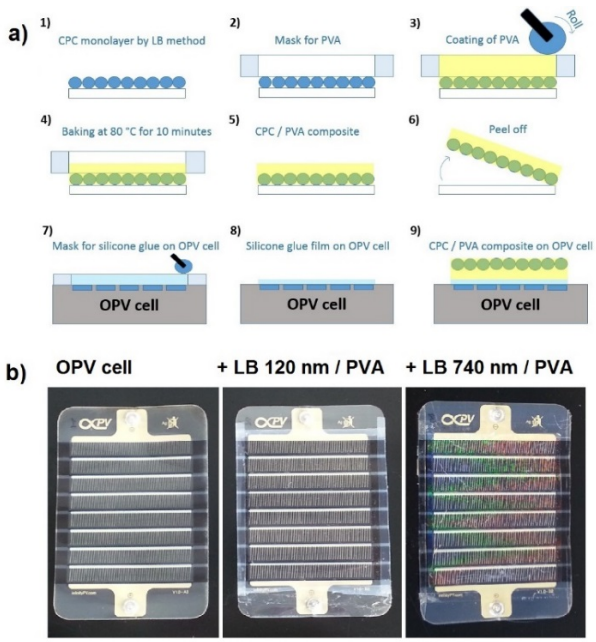

Fig. 1. A schematic shows the process of making LB monolayer / PVA composite (a), while the comparison of bare OPV cell and OPV cells covered with LB 120 nm / PVA and LB 740 nm / PVA composites is shown in (b).

The process of formation of a CPC / PVA composite film and its subsequent transfer onto a new substrate is then shown in Fig. 1. The process included following steps: fabrication of a large-area CPC film on PES substrate, making a mask for coating of PVA glue (175 μm thick), coating the PVA glue film through a mask by a process resembling a simplified ink proofing (the glue by Stick.ie had a form of hydro-gel rather than a solution of PVA in water), baking the composite film at 80 °C for 10 minutes, cutting the dried composite film out of the mask and peeling it off. Two other steps were then utilized in order to robustly attach the freestanding composite films onto the organic photovoltaic (OPV) cells, namely masking and gluing. A mask was made for the silicone glue film (50 μm thick), the glue was added via the mask and then the film was dried for 2 minutes before attaching the freestanding CPC / PVA

Optical Materials EXPRESS

film 'sticker' onto the OPV cell. Figures 2(a)-2(d) shows the surface morphology of the original CPC films and the CPC / PVA composites in comparison.

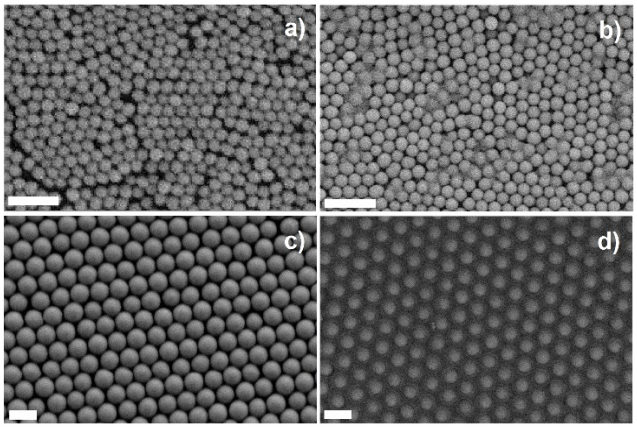

Fig. 2. The SEM micrographs depict the surfaces morphology of LB 120 nm (a) and LB 120 nm / PVA (b) films and LB 740 nm (c) and LB 740 nm / PVA (d) films in comparison. The scale bars correspond to 1 μm in all images.

The optical characteristics of the CPC films and their composites with PVA were measured using a Mikropack halogen HL2000 white light source, with a focused spot size at the sample of approximately 1.5 mm in diameter. The transmitted or reflected light was collected via an optical fibre connected to an Ocean Optics HR4000 detector for wavelengths in the UV–vis range. Spectral analysis was performed using Ocean Optics software SpectraSuite. Reflectance measurements were calibrated against a Thor Laboratories ME1-PO1 silver mirror in normal incidence arrangement. Transmission calibration was made with respect to air. Transmission spectra of the samples were acquired at the angle of incidence $\theta = 0°$ with respect to the film normal.

The conversion efficiency and other parameters of the OPV cells were determined from V-A characteristics using a Newport Oriel 91193 series 1600 W solar simulator and at conditions described in Ref. 19, where the incident spectrum was calibrated at 1000 W/m^2 using a reference cell. The stability of the light source was kept at ± 1.5% and the intensity corresponded to 1.5 AM over the entire surface area of the OPV cell. Data were recorded for bare OPV cells and the cells with the transferred photonic films at the angles 0°, 15°, 30° and 45° off from the normal with a help of a home-made sample holder securing the constant average distance of the cell from the source.

For testing the optical effects of CPC /PVA films on commercially available OPV cells we purchased the OPV modules of 5% power conversion efficiency (PCE) from DTU, Denmark. The technical note of the OPV cells, however, describes the cell active area may vary between 20 – 50 cm^2 where 5% PCE stands for the active area of 20 cm^2. The physical dimension of each OPV cell was 10 × 14 cm with an active area, i.e. stripes of absorbing layers covered by contact electrodes estimated to be ≈50 cm^2. This reduced the original 5% efficiency to 2% in our solar simulator results. The transferred films had to have a minimum size of ca. ≈72 cm^2 as their dimensions were based on the overall dimensions of the OPVs which included the separations between the stripes of the absorbing layers.

3. Results and discussion

The material choice for making the CPC films using PVA glue was inspired by previous studies [14–16] reporting the thin film transfer for layer-by-layer stacking of two- and three-dimensional CPC films by micro transfer printing. These techniques are useful when precise

Optical Materials EXPRESS

CPC film transfers are required and benefit from the use of micrometer or even sub-micrometer thicknesses as well as the adhesive properties of the PVA in the processing steps.

However, in this present work, our aim was simply to establish a simple, efficient, cheap and reliable process resulting in robust composite photonic material transfer involving CPC samples of large surface areas, which was also compatible with roll-to-roll processing of the CPC films so as to demonstrate the manufacturability of the process.

The transfer process for large surface area CPC films was optimized experimentally resulting in approx. ≈50 – 70 µm thick PVA films obtained after the baking process. We compromised demands on mechanical strength of films in terms of the choice of particular PVA material whilst maintaining the requirement of high transparency and low materials usage via the use of as thin a composite film as possible. We used commercially-available PVA glue which displayed gel-like properties, i.e. high viscosity. The mechanism of film drying occurs via cross-linking of the polymer with additives present in the glue rather than through solvent evaporation as reported e.g. in Ref. 15, although solvent evaporation also necessarily occurs. We appreciate that such glues may vary slightly with manufacturer but we suggest that these variations are unlikely to result in the failure of the general process outlined here.

In order to prove the versatility of the transfer method, we applied it first on 3D CPC films composed of organized arrays of silica and polystyrene (PS) nanospheres grown on polymer substrates. The refractive index of PVA baked at 80 °C for 10 minutes was n = 1.52, which was a value in between the values for silica spheres with n = 1.44 and for polystyrene spheres having n = 1.60, respectively. Figure 3 shows the optical reflectivity spectra of the bare and freestanding CPC / PVA composites assembled of 13-layer LB film of silica 250 nm particles, 30-layer controlled evaporation (CE) film [10] of silica 235 nm particles and 30-layer film of polystyren 265 nm particles grown by under oil vertical assembly (VA) method [17], for comparison. The red-shifted stop band centre positions were observed in the reflectivity spectra of the CPC / PVA composite films. In addition the amplitude of the stop bands observed for the composites were all lower than those of the respective bare CPCs. Both effects were associated with the change in the effective refractive index of the bare and the composite films from 1.348 to 1.475 for silica and from 1.467 to 1.579 for polystyrene and the refractive index difference reduced from 0.44 and 0.60 to approximately ≈0.08 for both types of composites, respectively. Interestingly an opposite effect on the amplitude, i.e. following an increase in the refractive index difference of transferred composite films has been reported elsewhere [18] for high index inorganic glass materials infilled in similar CPCs.

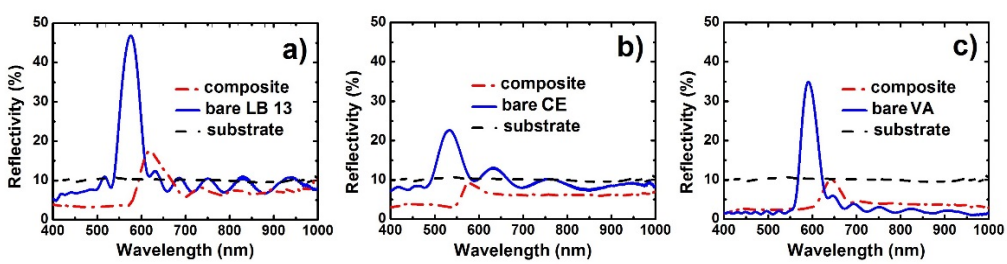

Fig. 3. The optical reflectivity spectra of colloidal crystal photonic multilayers (a) 13-layer LB multilayer of 250 nm silica particles, (b) controlled evaporation (see Ref. 10) multilayer of 235 nm silica particles and (c) vertical assembly grown multilayer of 265 nm polystyren particles in comparison with the spectra of freestanding composite films of the original films in PVA.

Figure 4(a) shows the optical reflectivity spectra of LB monolayers of silica particles with 120 nm diameter (LB 120 nm) and monolayers of silica particles with 740 nm diameter (LB 740 nm) in comparison with the spectra of the PES foil substrate and the PES substrate coated with 50 µm thick silicone glue film, respectively. The spectra reveal the differences between the two CPCs, being composed of ‘small’ and ‘large’ sized nanospheres. While the LB

Optical Materials EXPRESS

120 nm monolayer exhibited reduced reflectivity of about 5-7% in comparison with the PES substrate foil and of about 4-6% the PES substrate coated with a silicone glue film, the LB 740 nm monolayer exceeded the reflectivity of the PES substrate of about 5 – 7% in the visible wavelength range. When the LB 120 nm monolayer was then transferred onto an OPV cell by the process described here as shown in Fig. 1., the reflectivity of the OPV cell, recorded through the stack including the CPC / PVA composite, silicone film, double pouch foil, and active area with absorbing layer and array of electrodes - decreased again of about 5-7% as shown in Fig. 4(b). The reflectivity of the same stack including the LB 740 nm monolayer of silica particles changed only slightly compared to the reflectivity recorded for the bare OPV cell. These results suggest that for normal light incidence the LB 740 nm monolayer in PVA would not be optically active on an OPV cell but on the other hand the LB 120 nm monolayer should be. Figure 4(c) shows the transmittance through the active absorbing layer of the OPV cell. Most efficient photo-current generation may be expected in the range of 570-670 nm.

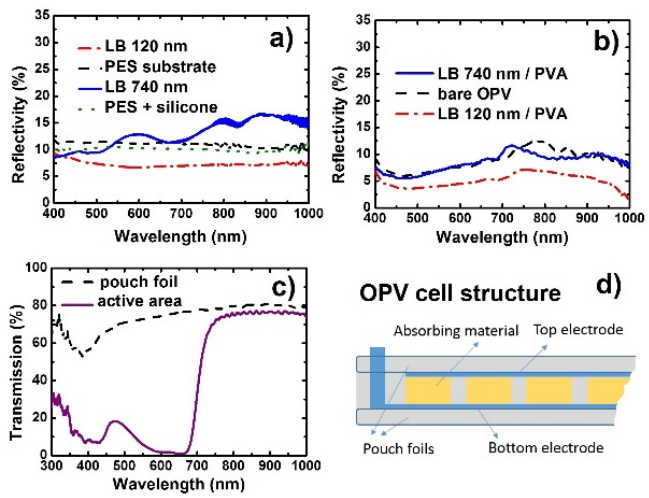

Fig. 4. The optical reflectivity spectra shown (a) LB 120 nm and LB 740 nm deposited on polyester foils in comparison with the reflectivity of the substrate and the reflectivity of the substrate coated with a silicon glue film; (b) those of (a) glued with a silicone glue film onto an OPV and (c) the optical transmittance of an OPV cell (d) measured through double pouch foil and in the active area.

Figures 5 and 6 show comparisons of the short-circuit current (I_{SC}), the open-circuit voltage (V_{OC}), the fill-factor (FF) and the power conversion efficiency (PCE) recorded from original OPV cells and the cells with the transferred LB 120 nm and LB 740 nm monolayers at the angles 0°, 15°, 30° and 45° off from the normal. The CPC / PVA films acted optically in different ways; the LB 120 nm / PVA film produced an anti-reflective effect resulting in the overall increase in the PCE of the cell of approx. + 5.2-8.3% depending on angle. The values of I_{SC}, I_{MP} in this case remained nearly constant while the V_{OC}, V_{MP} increased. An increase in the FF followed due to $FF = V_{MP}I_{MP}/V_{OC}I_{SC}$ with $\Delta V_{MP} \approx 2\Delta V_{OC}$.

In contrast, the LB 740 nm / PVA film exhibited nearly constant values of V_{OC} and V_{MP} at all measured angles and diffractive optical effects which were inefficient for normal and near normal light incidence but became more pronounced for higher off normal angles of the incidence. As a result, the PCE increased by + 3.0% in comparison to the values recorded at 30° and + 7.8% for values recorded at 45°, respectively. An increase in the PCE values at these angles followed an increase in the I_{SC}, I_{MP} values, where $\Delta I_{SC} \approx 1.4\Delta I_{MP}$, which was also responsible for the overall decrease in the FF.

Optical Materials EXPRESS

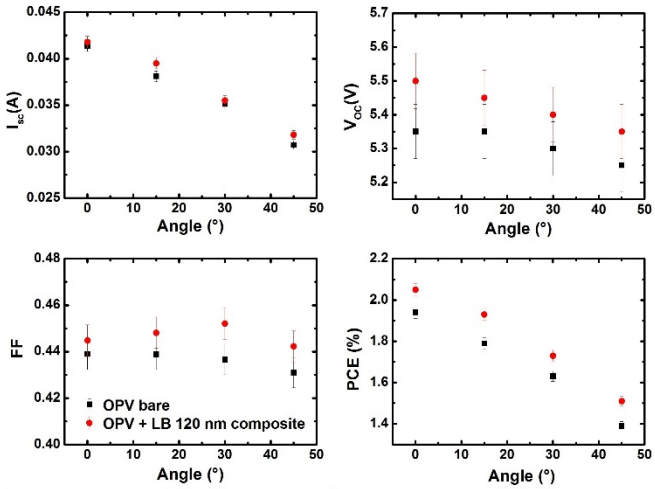

Fig. 5. Solar simulator data showing in comparison of the I_{SC}, V_{OC}, FF and PCE parameters recorded from an OPV cell before and after the transfer of LB 120 nm / PVA composite films (glued with a 50 μm thick silicone film).

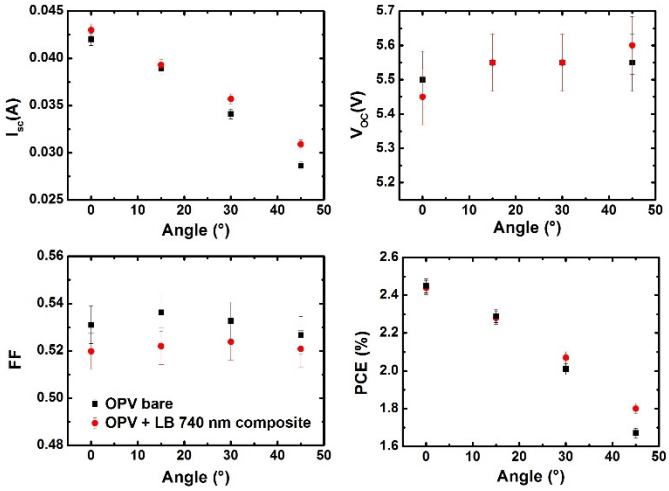

Fig. 6. Comparison of solar simulator data showing the I_{SC}, V_{OC}, FF and PCE parameters recorder from an OPV cell before and after the transfer of LB 740 nm / PVA composite films (glued with a 50 μm thick silicone film).

There are some issues we have to point out when comparing our results with those obtained using the best performing CPC-based anti-reflective coatings reported [20, 21]: (i), we achieved quite reasonable enhancement of the PCE for a composite LB 120 nm /PVA film, i.e. + 5-8% as compared to the 13% enhancement reported in Ref. 20 for materials based on the use of similar sized silica nanoparticles – considering the index difference benefit for bare CPC films, but we have also addressed concerns regarding the mechanical stability of the materials deployed; (ii) we used 120 nm and 740 nm nanoparticles with intention to demonstrate two different effects, i.e. the anti-reflective effect of small diameter particles and the diffractive effect of larger diameter particles. The particular particle diameters were selected after determining the optical transmission and reflectivity of various LB monolayers. The 120 nm particle films showed most pronounced improvement the transmission in the visible range among films made of 50, 87, 100, 120, 175, 210, 250 and 354 nm particles similarly as 740 nm particles exhibited most pronounced diffractive effect among the films

Optical Materials EXPRESS

made of 500, 600, 650 and 740 nm particles, respectively (iii), we have used commercial OPV cells with the size of 10 × 14 cm^2 which was already optimized (obviously) by the manufacturer in order to maximize its absorbance. This might make a comparison with the results achieved on home-made and mm-surface area cells [20] rather difficult to make since these almost always have major issues in terms of active surface area as well as stability. In contrast the OPV cells we used had excellent stability, i.e. their parameters remained unchanged within a period of 3 months which we have verified by repeated testing with an experimental error lower than ± 1.5%; (iv), we performed the cell testing on the same cell when comparing the results without and with the photonic 'sticker', which was often not the case in all reported experiments performed elsewhere. We consider this as crucial factor for securing reliable results since even commercial cells differ slightly in their performances.

We have demonstrated a potential of a new method designed to enhance the performance of real-sized commercial optoelectronic device such as thin film solar cells. As a result the option of using photonic film 'stickers' in a step following the fabrication process of a functional device seems to be quite commercially feasible. Such a layer could be easily attached and could even provide additional encapsulation, helping not only to enhance the performance of the device, but also to protect the delicate active layers from attack by moisture or oxygen, which are known to result in the rapid deterioration of device performance.

4. Conclusions

We have demonstrated a new way to fabricate and transfer the large surface area (>100 cm^2) flexible colloidal photonic crystal films from their original substrate to new substrates via a process involving the use of simple PVA glue which results in the fabrication of films having useful, exploitable optical properties and improved mechanical robustness as compared to the original films. The light trapping effects produced by monolayer CPC / PVA films were able to enhance the power conversion efficiency of real-sized, commercial organic photovoltaic cells by about 8% according to our solar simulator testing. We anticipate that the application of CPC films in various PV, OPV, OLED and even laser technologies will become widespread once the advantages of our new process are appreciated.

Funding

Science Foundation Ireland (15/IA/301); FP7 - Marie Curie IAPP 2012 (324449).

Acknowledgments

This work was funded by Science Foundation Ireland, project no. 15/IA/3015: 'Design, Deposition and Exploitation of Novel Micro and Nano-scale Materials and Devices for Advanced Manufacturing- DEPO-Man', and FP7 - Marie Curie IAPP 2012 (324449) project 'Assembling Langmuir-Blodgett Architectures Through the use of Roll-to-roll Systems – ALBATROSS'.

The authors thank Oliver Pemble for capturing SEM images of the CPC and CPC / PVA films.